Pr and Cu magnetism in $(Pr_{1.5}Ce_{0.5})Sr_2Cu_2MO_{10-\delta}$ (M=Nb, Ta): Correlations with a suppression of superconductivity

T. J. Goodwin and R. N. Shelton
Department of Physics, University of California, Davis, California 95616

H. B. Radousky
Lawrence Livermore National Laboratory, Livermore, California 94550
and Department of Physics, University of California, Davis, California 95616

N. Rosov and J. W. Lynn
Reactor Radiation Division, National Institute of Standards and Technology, Gaithersburg, Maryland 20899
(Received 2 May 1996; revised manuscript received 26 July 1996)

The magnetic properties of nonsuperconducting $(Pr_{1.5}Ce_{0.5})Sr_2Cu_2MO_{10-\delta}$ with M=Nb, Ta are characterized with dc magnetization, specific-heat, and neutron-diffraction experiments. Data for $(Pr_{1.5}Ce_{0.5})Sr_2Cu_2NbO_{10-\delta}$ reveal complex Cu magnetism marked by antiferromagnetic order below 200 K, spin structure transitions at 130 and 57 K, both collinear and noncollinear antiferromagnetic spin structures, and weak ferromagnetic behavior below 130 K. The data also indicate an anomalous ordering of the Pr spins near 10 K, a large linear contribution to the low-temperature specific heat, and a Pr $4f$ crystal-field ground state similar to that found in $PrBa_2Cu_3O_7$. Furthermore, there is evidence that the weak ferromagnetic behavior couples to the Pr ordering near 10 K. Identical Pr magnetism and similar Cu magnetism are found in $(Pr_{1.5}Ce_{0.5})Sr_2Cu_2TaO_{10-\delta}$, deoxygenated $(Pr_{1.5}Ce_{0.5})Sr_2Cu_2NbO_{10-\delta}$, and deoxygenated $(Pr_{1.5}Ce_{0.5})Sr_2Cu_2TaO_{10-\delta}$. These results indicate that superconductivity is suppressed in these compounds in the same phenomenological manner as in $PrBa_2Cu_3O_7$. We interpret this as evidence that superconductivity is suppressed by the same mechanism in both structures and propose that a general correlation exists between anomalous Pr magnetism and a lack of superconductivity in these Pr-based high-T_C cuprates. The significance of these results and analyses to understanding and modeling the suppression of superconductivity by Pr in high-T_C cuprates is discussed. [S0163-1829(97)03505-4]

I. INTRODUCTION

One of the most enigmatic and controversial problems in the field of high-temperature (high-T_C) superconductivity is the suppression of superconductivity by the Pr ion in the $RBa_2Cu_3O_7$ (RBCO) structure.[1] This suppression is unconventional and is accompanied by other properties that are also anomalous for the RBCO compounds such as a Pr Néel temperature (T_N) two orders of magnitude larger than expected, an unexpected insulating electronic state, and evidence of strong interaction between the Pr $4f$ and CuO_2 planar electronic states. PrBCO also shows a pseudotriplet Pr $4f$ crystal-field (CF) ground state marked by three broad and closely spaced energy levels which yield magnetic data that simulate a Curie-Weiss profile for a Pr ion with a reduced effective moment (μ_{eff}),[2] and a large linear contribution to the low-temperature specific heat.[3] The underlying mechanisms responsible for the suppression of superconductivity and the other anomalous properties of PrBCO are not well understood and are controversial.[1,4] Thus, no specific model has yet gained full acceptance. However, it is apparent that f-electronic interactions play a key role in determining the properties of PrBCO.[1] Furthermore, in high-T_C compounds where the presence of Pr does not affect superconductivity, such as $(Pr_{1.83}Ce_{0.17})CuO_4$ or $Bi_2Sr_2(Ca_{1-x}Pr_x)Cu_2O_8$, Pr does not show anomalous magnetism, the Pr ion has a conventional singlet CF ground state and there is no evidence of interaction between the Pr $4f$ and CuO_2 planar electronic states.[1] This suggests that the anomalous properties of PrBCO are related to the suppression of superconductivity.[1] Hence, current attempts to understand and model this suppression tend to focus on the anomalous properties of PrBCO and the relationships among Pr magnetism, f-electron interactions, an insulating electronic state, and the suppression of superconductivity.[1,4]

Recent characterizations of the isostructural $(R_{1.5}Ce_{0.5})Sr_2Cu_2NbO_{10-\delta}$ (RCSCNO) family of compounds (which forms for R=Pr, Nd, Sm, Eu, and Gd) suggest that PrCSCNO may be a second example of a high-T_C compound in which the Pr ion suppresses superconductivity, shows anomalous magnetism, shows a reduced effective moment, and induces an insulating state while all other members of the structure are superconducting.[5–9] The phenomenological similarities to PrBCO suggest that Pr suppresses superconductivity in PrCSCNO by the same unconventional mechanism found in PrBCO, and that PrCSCNO affords another system by which to study this mechanism. However, these preliminary results and analyses are incomplete and ambiguous particularly in light of recently reported measurements on PrCSCNO which show irreversibilities and multiple transitions in the magnetic data, and no evidence of Pr ordering in the specific-heat data.[9] This leaves the overall magnetic state as well as the issue of Pr magnetism and its relationship

to the suppression of superconductivity in PrCSCNO unresolved.

In this paper, we examine the magnetic properties of PrCSCNO, the Ta analog $(Pr_{1.5}Ce_{0.5})Sr_2Cu_2TaO_{10-\delta}$ (PrCSCTO), deoxygenated PrCSCNO, and deoxygenated PrCSCTO with neutron diffraction, dc magnetization (M_{dc}), and specific-heat measurements. We remove the ambiguities surrounding the properties of PrCSCNO and demonstrate that PrCSCNO exhibits anomalous Pr magnetism which is comparable to the Pr magnetism in PrBCO. We also show that the unusual behavior of the magnetic data of PrCSCNO is due to complex Cu magnetism marked by antiferromagnetic (AF) order, multiple spin structure transitions, both collinear and noncollinear spin structures, and weak ferromagnetic behavior. In addition, PrCSCTO, deoxygenated PrCSCNO, and deoxygenated PrCSCTO are found to exhibit identical Pr and similar Cu magnetic behavior as PrCSCNO. Based upon these results, we propose that there exists a subclass of nonsuperconducting Pr-based high-T_C cuprates, and that a general correlation exists between anomalous Pr magnetism and a suppression of superconductivity in this subclass. Finally, the relevance of these results to understanding and modeling this suppression of superconductivity is discussed.

II. EXPERIMENT

Samples of PrCSCNO, PrCSCTO, and EuCSCNO were prepared by standard solid-state reaction methods. Portions of the samples were deoxygenated by firing in a flowing argon atmosphere at 700 °C for 2 days; deoxygenated samples are designated *d*-PrCSCNO and *d*-PrCSCTO. Powder x-ray-diffraction (XRD) data were collected with a Siemens D500 x-ray diffractometer using Cu $K\alpha$ radiation. Structural parameters were determined from Reitveld refinements of the XRD data to the reported *R*CSCNO *I*4/*mmm* structure.[5,10,11] Thermogravimetric (TGA) similar to that used by Cava *et al.* on NdCSCNO (Ref. 7) was used to determine the oxygen stoichiometry of the samples. Details of sample preparation, deoxygenation, XRD, structural refinements, and TGA are given in Refs. 10 and 11. Neutron-diffraction data were collected with the BT-2 and BT-9 triple-axis neutron spectrometers of the NIST Research Reactor. Neutrons with an incident wavelength of 0.235 nm were reflected from a pyrolytic graphite 002 monochromator and scattered from about 10 g of powder PrCSCNO in a cylindrical holder. Collimation before the monochromator, after the monochromator, and after the sample was typically 60′. The scattered neutrons were detected with no energy analysis and no preferred orientation of the powder was observed in the data. $M_{dc}(T,H)$ data were collected with the Quantum Design MPMS superconducting quantum interference device magnetometer equipped with a 55 kOe magnet. Specific-heat data were collected from ~0.6 to 60 K with a standard adiabatic heat-pulse calorimeter attached to a He^3 cryostat.

III. RESULTS AND ANALYSES

The XRD data for the samples showed diffraction patterns consistent with that expected from the *I*4/*mmm* *R*CSCNO structure (Fig. 1).[5,6,10,11] Several weak peaks in the data that could not be indexed to the *R*CSCNO structure indicated the presence of $RSr_2Cu_2MO_8$, $Sr_2(RM)O_6$, and $Sr(M_{1-x}Cu_x)O_3$ impurities where R=Eu or Pr and M=Nb or Ta. Monitoring the intensities of these weak peaks as various quantities of these impurities were deliberately mixed with portions of the samples confirmed their origin. Further analysis demonstrated that the presence of the impurities could be detected to better than 1 f.u. % with our XRD measurement technique. Based on these results, we determined that the samples were better than 98% pure.[10,11] Table I summarizes refined lattice parameters and oxygen stoichiometry from

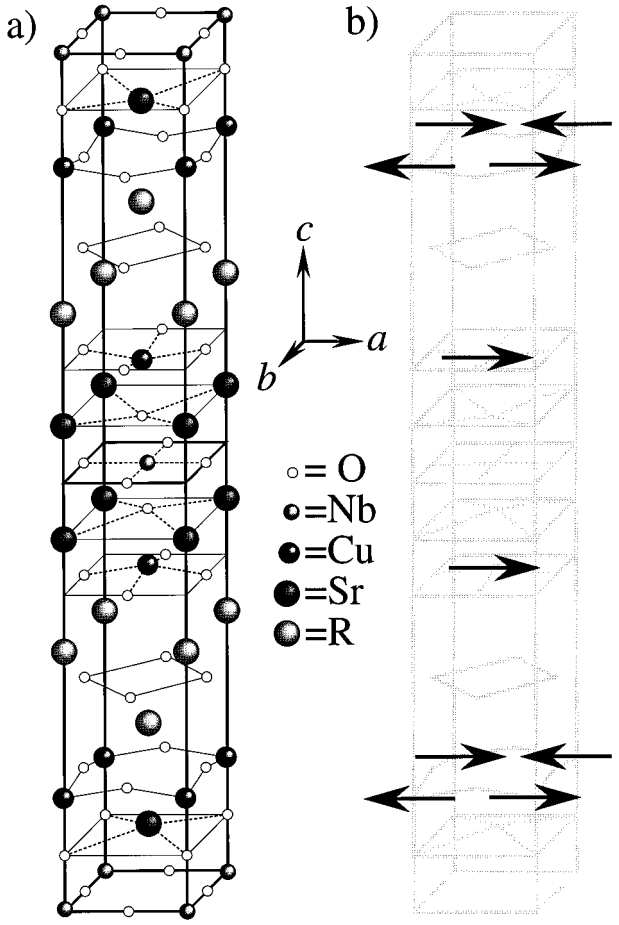

FIG. 1. (a) The crystal structure for the $(R_{1.5}Ce_{0.5})Sr_2Cu_2NbO_{10-\delta}$ compounds. (b) Illustration of the $+--+$ Cu spin structure proposed in the text with the Cu spins aligned parallel to the *a* axis.

TABLE I. Structural parameters and δ's for the samples used in this work.

Compound	*a* (nm)	*c* (nm)	δ
PrCSCNO	0.388 73(9)	2.8761(6)	0.046(3)
d-PrCSCNO	0.389 24(6)	2.8846(1)	0.162(6)
PrCSCTO	0.388 51(2)	2.8844(3)	0.048(3)
d-PrCSCTO	0.388 99(6)	2.8909(9)	0.115(5)
EuCSCNO	0.386 63(1)	2.8755(8)	0.047(3)

TGA results for the samples. Lattice parameters for PrCSCNO and EuCSCNO agree with previously reported values.[6,7] Results for *d*-PrCSCNO and *d*-PrCSCTO reveal an expansion of the lattice which accompanies the deoxygenation of the parent compounds. The values found for δ in EuCSCNO, PrCSCNO, and PrCSCTO are nearly identical. Together with recent electron-energy-loss spectroscopy (EELS),[12] specific-heat results,[11,13] and structural analysis[6,10,11] on the $(Eu_{1.5-x}Pr_xCe_{0.5})$SCNO system—which indicate that the Pr ion is in a +3 valence state and the Ce ion is a +4 valence state in these compounds—these values of δ give a carrier count between 0.21 to 0.20 holes per Cu ion in EuCSCNO, PrCSCNO, and PrCSCTO from a straightforward valence count. However, resistivity and magnetic measurements on these samples[11,13] confirm that PrCSCNO and PrCSCTO are insulating, while EuCSCNO and all other *R*CSCNO and *R*CSCTO compounds are metallic and superconducting. These results indicate that as with PrBCO, there is no clear reason for PrCSCNO and PrCSCTO to be insulating.[6,11,13] Finally, both resistivity and $M_{dc}(T)$ data at $H=10$ Oe confirm that the EuCSCNO sample is metallic and is superconducting with a T_C of 27 K and a superconducting volume fraction near 30%. These properties of the EuCSCNO sample are reported in detail elsewhere[11,13] and are comparable to previously reported results.[6]

Close inspection of the neutron-diffraction pattern of PrCSCNO below 200 K revealed several weak temperature-dependent peaks that could not be accounted for by structural refinements. Figure 2 shows diffraction patterns for $21.5°\leqslant 2\theta \leqslant 27.5°$ at several temperatures between $T=40$ and 160 K. The two peaks below ~24° were temperature independent and we attribute them to impurities. The temperature-dependent peaks observed above 24° may be indexed as 1/2 1/2 0, 1/2 1/2 1, and 1/2 1/2 2 reflections, and we attribute them to magnetic order in PrCSCNO. Due to the complexity of the magnetism, multiple transitions, a small ordered moment, and the complicated crystal structure, we were restricted to analyzing these 1/2 1/2 *l* magnetic peaks since they were the only ones not obscured by nearby sample or impurity structural peaks. Hence, the information we can obtain from neutron diffraction on this powder PrCSCNO sample is limited.

The temperature dependence of the 1/2 1/2 1 and 1/2 1/2 2 peak intensities are shown in Fig. 3. The data indicate an onset of the magnetic peaks above 200 K and two sudden redistributions of the peak intensities near 130 and 57 K. The onset of the magnetic peaks is difficult to determine due to the extremely weak scattering at higher temperatures. However, the magnetic peaks observed below 200 K were not detected at 300 K. The presence of 1/2 1/2 *l* reflections at high temperatures implies, and leads us to conclude, that the Cu spin configuration is AF in the CuO_2 planes as is observed in all other high-T_C cuprate systems,[14] where nearest-neighbor Cu spins within a CuO_2 plane are antiparallel and all the Cu spins are parallel to the *a*-*b* plane. The sudden changes in peak intensities near 130 and 57 K indicate reorientations of the spin structure at these temperatures. This yields three distinct spin structures for PrCSCNO with temperature regions from T_N (above 200 K) down to 130 K (phase I), 130 to 57 K (phase II), and below 57 K (phase III). However, the presence of the 1/2 1/2 *l* peaks for all three

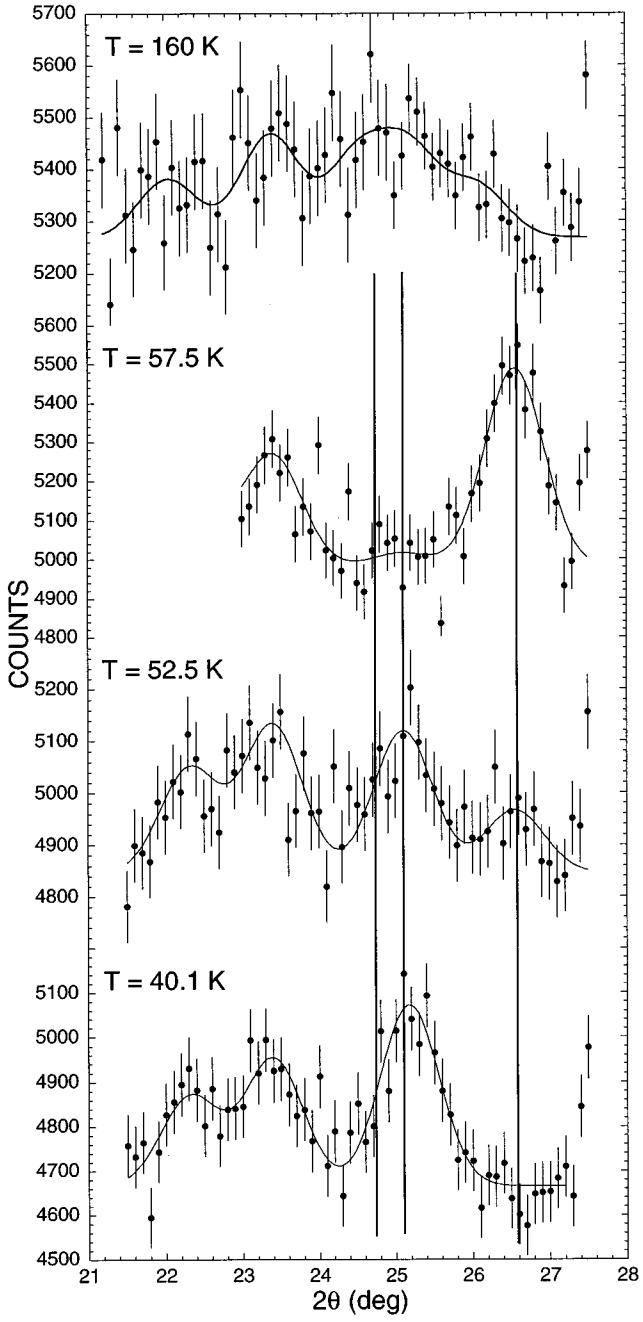

FIG. 2. The observed neutron-diffraction pattern over the range of $21.5°\leqslant 2\theta \leqslant 27.5°$ for temperatures between 40 and 160 K. The bottom three patterns are in the vicinity of the magnetic anomaly at 57 K. The pattern for $T=160$ K shows the scattering characteristic of the collinear Cu spin structure above 130 K. The peaks at $2\theta=22.3°$ and 23.4° are temperature independent and are probably due to impurities. The extended vertical lines indicate the position of the 1/2 1/2 0, 1/2 1/2 1, and 1/2 1/2 2 reflections for $T\approx 50$ K. The peaks at 160 K are shifted to slightly lower angles due to the thermal expansion of the sample.

phases indicate that the proposed CuO_2-planar AF spin structure is present in all three spin structures. Finally, the 57 K transition coincides with the ~57 K cusp reported in the $M_{dc}(T)$ of PrCSCNO,[6,9] which indicates that the 57 K cusp is the magnetic signature of the 57 K spin structure transition.

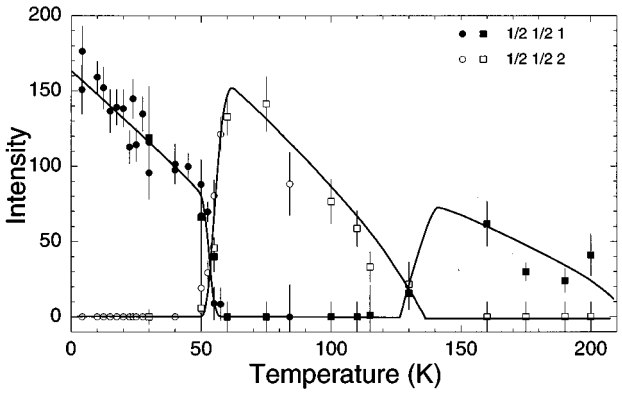

FIG. 3. Temperature dependence of the 1/2 1/2 1 and 1/2 1/2 2 neutron-diffraction peaks showing the spin structure transitions at 55 and 130 K. The solid lines are a guide to the eye.

Determination of the magnetic structure along the c axis is more problematic. The unit cell of PrCSCNO contains two pairs of CuO_2 planar bilayers; each bilayer shifted by $1/2(\mathbf{a}+\mathbf{b})$ from the next[5,6,10,11] (Fig. 1). These four CuO_2 layers are located at $z=z_0$, $1/2-z_0$, $1/2+z_0$, and $-z_0$ in the unit cell with $z_0 \approx 0.1425$,[6,10,11] and bilayers consisting of the $1/2-z_0$, $1/2+z_0$ and z_0, $-z_0$ plane pairs. The structure factor for an hkl reflection from a collinear spin configuration is

$$F_{hkl}=\sum_j p_j \mu \exp\{2\pi i(hx_j+ky_j+lz_j)\}, \qquad (1)$$

where $p_j=\pm 1$ is the configuration of the jth spin; μ is the magnetic moment; x_j, y_j, and z_j are the fractional coordinates of the Cu ions. Summing over all Cu moments in the magnetic unit cell and equivalent reflections, we find the ratio of the 1/2 1/2 1 to 1/2 1/2 2 peak intensities is

$$R=\frac{F^2_{1/2\ 1/2\ 1}}{F^2_{1/2\ 1/2\ 2}}=\frac{1+1/2\ \ P\ \cos 4\pi z_0}{1+1/2\ \ P\ \cos 8\pi z_0}. \qquad (2)$$

$P=P_1P_4+P_2P_3$ describes the c-axis stacking spin configuration, where P_j is 1 for the jth plane if the spins are parallel to those in the reference plane and -1 if the spins are antiparallel. P can be ± 2 depending upon the c-axis stacking. A $+-+-$ stacking (spins in the z_0, $1/2-z_0$, $1/2+z_0$, $-z_0$ planes aligned parallel, antiparallel, parallel, antiparallel relative to the reference plane) gives $P=-2$ and $R=0.64$. For a $+--+$ stacking, $P=+2$ and $R=8.2$. The ratios of the 1/2 1/2 0 to 1/2 1/2 2 peak intensities were determined in a similar manner and the ratios of the 1/2 1/2 0 and 1/2 1/2 1 to the 1/2 1/2 2 peak intensities for the possible collinear spin configurations of this structure were computed. Normalized calculated and observed peak intensity ratios are summarized in Table II; calculated peak intensity ratios include the effect of the Cu^{+2} magnetic form factor and the Lorentz factor for powder peaks. From Table II, we see that the peak intensity ratios in the high-temperature phase ($T>130$ K) are consistent with a $+--+$ or $++++$ collinear c-axis stacking; a $+--+$ collinear configuration with the spins parallel to the a axis is illustrated in Fig. 1(b). However, between 130 and 60 K, the 1/2 1/2 1 reflection is suppressed relative to the 1/2 1/2 2 reflection and there is no collinear spin structure which corresponds to these results. Similarly, below 50 K, the spin structure cannot be simple collinear since both the 1/2 1/2 0 and 1/2 1/2 2 reflections are very weak relative to the 1/2 1/2 1 peak. Hence, we conclude that the spin structures below 130 K are noncollinear.

TABLE II. Calculated 1/2 1/2 l peak intensity ratios for various collinear Cu spin stacking sequences along the c axis and observed intensity ratios at various temperatures for PrCSCNO. Calculations include the effect of the Cu^{+2} magnetic form factor and the Lorentz factor for powder peaks.

	Calculated		Observed		
hkl	$[+-+-]$ or $[++--]$	$[+--+]$ or $[++++]$	40 K	57.5 K	160 K
1/2 1/2 0	0	1	0	0	1
1/2 1/2 1	0.63	0.76	1	0.07(9)	0.8(2)
1/2 1/2 2	1	0.10	0.0(1)	1	0.3(2)

We mention that below 20 K where an ordering of the Pr spins is suspected,[6] we are unable to unambiguously address Pr magnetism with our neutron-diffraction measurements at this time due to a low ordered moment and the complex magnetism of PrCSCNO. In addition, we found no evidence in the data for the Cu spin reorientation below 20 K proposed by Felner *et al.* for PrCSCNO.[9] Finally, in the absence of information on the magnetic structure of PrCSCNO, Felner *et al.* attributed a 57 K cusp in the magnetic data of PrCSCNO to an AF ordering of the Cu spins.[9] Our results indicate that this interpretation is incorrect and that the Cu T_N occurs above 200 K, while the 57 K magnetic cusp is related to a reorientation of the Cu spin structure.

Field-cooled and zero-field-cooled $M_{dc}(T)$ data at an applied field H of 10 Oe for PrCSCNO [Fig. 4(a)] show the large irreversibilities below 80 K and two cusps at 15 and 57

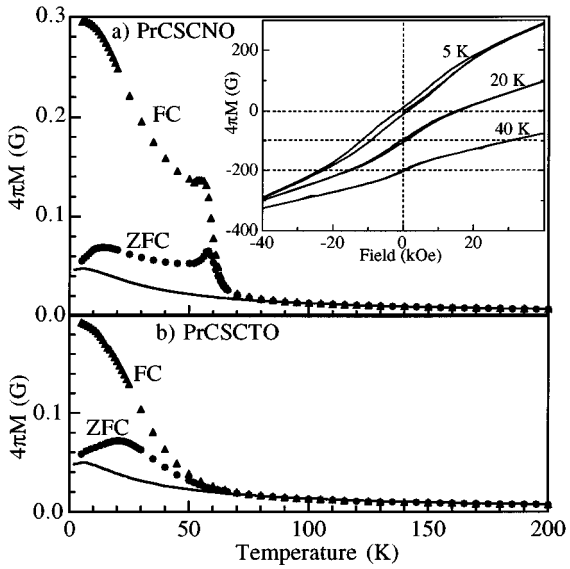

FIG. 4. Zero-field cooled and field-cooled $M_{dc}(T)$ data at $H=10$ Oe for (a) PrCSCNO and (b) PrCSCTO. The solid lines are the contribution of the Pr ions calculated from $\chi_d(T)$. Inset shows hysteresis loops for PrCSCNO—loops are offset by 100 G increments for clarity.

K that have been previously reported.[6,9] The 57 K cusp coincides with the transition near 57 K in the neutron-diffraction data indicating that the cusp is a magnetic signature of the transition. M_{dc} data as functions of time and field strength reveal hysteresis [inset of Fig. 4(a)] and relaxations of the field-cooled M_{dc} and remnant magnetization which are associated with the irreversibilities. The saturation field H_S of the hysteresis is ~21 kOe at 2 K and decreases monotonically with increasing temperature, and $M_{dc}(H)$ is linear above H_S at all temperatures. These irreversibilities, relaxations, and hysteresis are reminiscent of the weak ferromagnetic (WF) behavior of the Cu spins observed in La_2CuO_4,[15] and some R_2CuO_4 T' cuprates such as Gd_2CuO_4, Y_2CuO_4, and Tb_2CuO_4.[16–18] WF behavior in these T and T' structured cuprates has been attributed to a canting of the Cu moments away from strictly AF alignment under the influence of asymmetric exchange interactions as discussed by Dzyaloshinsky and Moriya.[19] The orthorhombic phase of La_2CuO_4 allows for such asymmetric interactions and supports a theoretical basis for this explanation.[20] But in the tetragonal T' cuprates, such asymmetric couplings cancel due to the square planar Cu-O coordination.[16,18,19] Hence, part of the basis of this interpretation of the origin of WF behavior in the T' structured cuprates is an assumption that the Cu-O coordination is not square planar due to local distortions of the crystal structure.[16–18] However, there is to date no clear evidence of such local structural distortions. Furthermore, the nature of these would-be distortions is unclear and a theoretical basis for the existence of WF under these circumstances has yet to be established.[16–19] Nevertheless, work in this area continues in order to understand the microscopic origins of the WF,[16–18] and it is clear that the WF behavior in these T' cuprates is associated with the Cu spins.[16,18] Since PrCSCNO and the R_2CuO_4 T' cuprates are of the same class of materials, have similar crystal structures,[6,10,11] and the phenomenology of the WF in these two structures is similar, it is reasonable to assume that the WF behavior of the two structures is the same general phenomenon and has the same origin. Though, as with the T' compounds, the tetragonal structure of the RCSCNO compounds does not allow asymmetric interactions. Therefore, by classifying the WF of PrCSCNO with that of the T' compounds, the same uncertainties regarding the origins of the WF and the issue of local structural distortions in the R_2CuO_4 T' compounds are generalized and apply to PrCSCNO as well.

Due to the (inherited) relevance of structural distortions to the WF behavior in PrCSCNO, we point out that the local structure of PrCSCNO is an open issue at this time. Although the refinements of the XRD data indicated that the RCSCNO $I4/mmm$ structure generally describes the structure of these compounds, the oxygen sites in the SrO and NbO_2 planes showed thermal parameters larger than physically possible,[10,11] implying structural irregularities for the oxygen sites in these planes. This suggests that these compounds suffer from the same rotation distortion reported by Zandbergen *et al.* for NdCSCNO where the NbO_6 octahedras are slightly rotated about the c axis.[21] Furthermore, the structural refinements of our neutron-diffraction data for PrCSCNO have indicated that the $I4/mmm$ space group does not adequately describe the crystal structure of PrCSCNO and confirm that the NbO_6 octahedras are distorted by a rotation about the c axis. These results have left the exact crystal structure of PrCSCNO uncertain until further measurements and analyses can be performed. Hence, local structural distortions and their relevance to the WF behavior in PrCSCNO remain unresolved issues at this time.

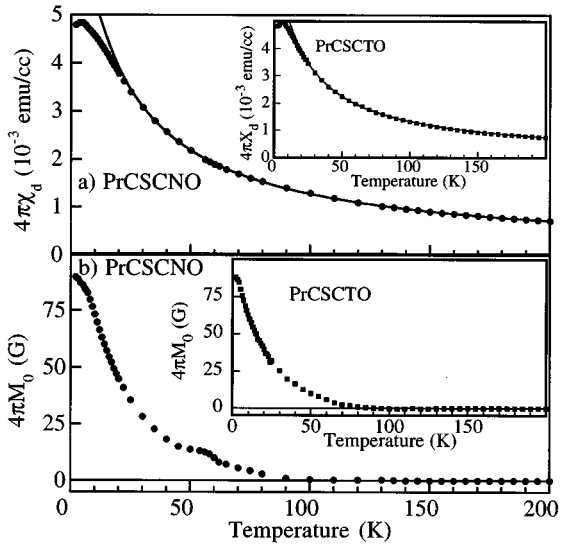

FIG. 5. (a) Differential susceptibility data for PrCSCNO and PrCSCTO (inset)—solid lines represent the Curie-Weiss fits of the data. (b) Remnant magnetization for PrCSCNO and PrCSCTO (inset).

In the R_2CuO_4 T' compounds that show WF behavior, the contribution of the rare-earth ions to the magnetic susceptibility is usually determined from the slope of the $M_{dc}(H)$ at fields large enough to saturate the WF (Refs. 16, 17, and 18) after the technique employed by Cooke, Martin, and Wells on the orthoferrites.[22] Applying this technique to PrCSCNO, $M_{dc}(T,H)$ for PrCSCNO is expressed to first order in a mean-field approximation with $H>H_S$ and $T<200$ K as

$$M_{dc}(T,H)=M_S(T)+[H+H_i(T)]\chi_d(T). \tag{3}$$

$M_S(T)$ is the contribution of the saturated WF, $H_i(T)$ is the internal field due to $M_S(T)$, and $\chi_d(T)=\chi_0+C/(T-\theta)$ is the linear differential susceptibility where χ_0 is the contribution of the core electrons and $C/(T-\theta)$ is the Curie-Weiss contribution of the Pr ions. The contribution from the AF-ordered components of the Cu moments is assumed to be negligible, and based upon recent EELS results for PrCSCNO,[12] the Ce ion is taken to be nonmagnetic. Following this analysis, $M_{dc}(H)$ data for PrCSCNO were collected for $H>H_S$ ($H=30$, 35, 40, 45, 50, and 55 kOe) between 2 and 300 K. For these temperatures and fields, the data were linear and reversible. Subsequently, for fixed T the data were fit to

$$M_{dc}(T,H)=M_0(T)+H\chi_d(T), \tag{4}$$

where

$$M_0(T)=M_S(T)+H_i(T)\chi_d(T) \tag{5}$$

is the field-independent remnant magnetization.

Values found for $M_0(T)$ and $\chi_d(T)$ are plotted in Fig. 5.

TABLE III. Results of fits of $\chi_d(T)$ data to a Curie-Weiss profile, $\chi_d(T)=\chi_0+C/(T-\theta)$, for 40 K$<T<$200 K. The goodness-of-fit is represented by the reduced chi square χ^2_ν.

Compound	χ_0 (emu/cc)	C (K emu/cc)	μ_{eff} (μ_B)	θ (K)	χ^2_ν
PrCSCNO	$5.58(6)\times10^{-6}$	0.0113(1)	2.82(4)	−16.9(4)	0.000 11
d-PrCSCNO	$1.36(2)\times10^{-5}$	0.0114(1)	2.81(2)	−15.4(6)	0.000 15
PrCSCTO	$4.9(2)\times10^{-6}$	0.0117(2)	2.87(2)	−19(1)	0.000 21
d-PrCSCTO	$1.2(3)\times10^{-5}$	0.0114(5)	2.84(5)	−16(2)	0.000 43

We see that $M_0(T)$ is essentially zero above 100 K and increases monotonically below 100 K with decreasing temperature. In addition, two cusplike features are observed near 57 and below 15 K. Closer inspection of the data revealed small but discernible nonzero values for $M_0(T)$ up to 120 K that are not evident in the plot. The nonzero $M_0(T)$ values below 120 K and the feature at 57 K reflect the irreversibilities and 57 K cusp in the $M_{\text{dc}}(T)$ data of Fig. 4(a). In addition, the onset of a remnant magnetization at 120 K appears to coincide with the 130 K spin structure transition seen in the neutron-diffraction data. This implies that the WF behavior is a feature of the spin structures below 130 K. Furthermore, the relevance of local structural distortions to the WF behavior raises suspicion that a subtle structural transition coincides with the 130 K spin structure transition. However, the relationships between crystal structure, spin structure, and WF behavior in PrCSCNO and high-T_C cuprates in general are uncertain at this point and leave considerable leeway for interpretation of the data. We therefore leave assessments of these relationships to future work. Finally, we mention that although $H_i(T)$ and $M_S(T)$ are important characteristics of the magnetic state of PrCSCNO, the relationship between $H_i(T)$ and $M_S(T)$ in Eq. (5) makes it difficult to determine each separately. In special cases for some R_2CuO_4 T' compounds $H_i(0)$ and $M_S(0)$ were determined.[16,17] Unfortunately, for PrCSCNO (and PrCSCTO) no special cases were found and we were unable to determine $H_i(T)$ and $M_S(T)$ separately at any temperature.

The $\chi_d(T)$ data for PrCSCNO [Fig. 5(a)] show a Curie-Weiss profile above 30 K with no deviations at 57 K. Together with the 57 K feature in $M_0(T)$, these results indicate that the 57 K transition is due exclusively to the Cu spins and does not directly involve the Pr spins. Below 10 K, the $\chi_d(T)$ data show a cusp with an apex at ~7 K, suggesting an ordering of the Pr sublattice. Since the $M_0(T)$ and hysteresis data below 7 K show no features or changes that can be associated with this cusp, we propose that the ordering is AF in nature. The $\chi_d(T)$ data for 40 K$<T<$200 K were fit to a Curie-Weiss profile, $\chi_d(T)=\chi_0+C/(T-\theta)$, and the results are summarized in Table III. χ_0 is small as expected and θ indicates an AF ground state for the Pr ions. Additionally, C yields a Pr μ_{eff} of $2.82\mu_B$ which is intermediate to the μ_{eff} expected from a Pr^{+3} and Pr^{+4} ion and is comparable to the reduced μ_{eff} of PrBCO. This may indicate that the Pr ion is in a mixed valence state in PrCSCNO. However, in light of recent EELS,[12] structural,[6,10,11] and our specific-heat measurements (below) which indicate that the Pr ion is in a +3 valence state in PrCSCNO, a more agreeable interpretation is that a Pr^{+3} ion in PrCSCNO has a $4f$ CF ground state comparable to that of PrBCO—giving rise in a similar fashion to a reduced Pr μ_{eff}.[2]

It is interesting to note that although the close proximity of the 13 K $M_{\text{dc}}(T)$ cusp and 7 K $\chi_d(T)$ cusp might suggest that they have the same origin, there are still significant dichotomies in the profiles and positions of the two cusps. The contribution of the Pr ions to the $M_{\text{dc}}(T)$ data, computed from $\chi_d(T)$, is shown as a solid line in Fig. 4(a). Comparison of the data shows that the Pr magnetism cannot generally account for the 13 K cusp and that no direct contribution from the 7 K Pr cusp can be discerned in the $M_{\text{dc}}(T)$ data. This suggests that the 13 K cusp in the $M_{\text{dc}}(T)$ data is a feature of the Cu magnetism that eclipses the contribution of the Pr magnetism and dominates the low-temperature behavior of the $M_{\text{dc}}(T)$ data. In order to investigate the relationship between the two cusps more carefully, zero-field-cooled $M_{\text{Cu}}(T)$ data for PrCSCNO were collected at various fields and are shown in Fig. 6 in terms of $M_{\text{Cu}}(T)/H$ together with the PrCSCNO $\chi_d(T)$ data of Fig. 5(a). As before, the $\chi_d(T)$ data were taken to represent the contribution of the Pr ions to $M_{\text{dc}}(T)/H$—even at low fields given the linearity of $\chi_d(T)$ at the higher fields—and we express $M_{\text{dc}}(T)/H$ as

$$M_{\text{dc}}(T)/H=\chi_d(T)+M_{\text{Cu}}(T)/H, \tag{6}$$

where $M_{\text{Cu}}(T)$ is the contribution of the Cu magnetism to $M_{\text{dc}}(T)$ and is equal to $M_S(T)$ for $H>H_S$ as discussed above. Figure 6 shows that the 13 K $M_{\text{dc}}(T)$ cusp (and the 57 K cusp) is nonlinear and is suppressed with increasing field strength, that there is a significant contribution to $M_{\text{dc}}(T)$ below 80 K from $M_{\text{Cu}}(T)$ which overshadows the contribution from the Pr ions, and that the 13 K cusp (and the 57 K cusp) cannot be accounted for by the Pr magnetism.

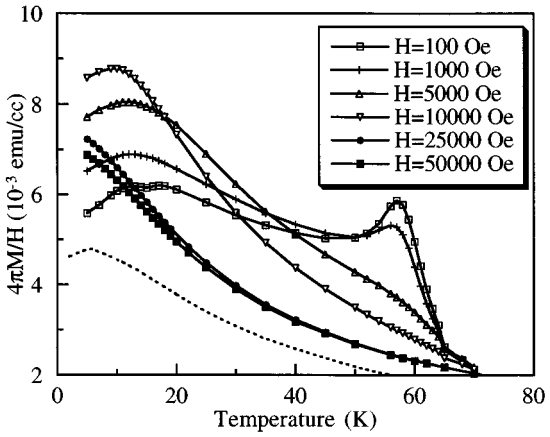

FIG. 6. Zero-field-cooled $M_{\text{dc}}(T)/H$ data for PrCSCNO at $H=100$ Oe, 1, 5, 10, 25, and 50 kOe. The dashed line represents the contribution of the Pr moments to the data through the $\chi_d(T)$ data.

Furthermore, for $H>21$ kOe—the maximum $H_S(T)$ measured above—the nonlinear 13 K cusp appears to be suppressed completely while a relatively field-independent bend stands out below 10 K. This bend presumably reflects both the 7 K cusp in the $\chi_d(T)$ data and a similar bend in the $M_0(T)$ data of Fig. 5(b). Assuming that the WF behavior dominates $M_{\mathrm{Cu}}(T)$, these results indicate that the 13 K $M_{\mathrm{dc}}(T)$ cusp in Fig. 4(a) is composed of a linear contribution from $\chi_d(T)$ plus a nonlinear 13 K cusp from $M_{\mathrm{Cu}}(T)$, and that the nonlinear 13 K cusp originates from features in the WF behavior. Hence, the profile, position, magnitude, field dependence, and nonlinearity of the 13 K cusp clearly distinguish it from the 7 K $\chi_d(T)$ cusp and indicate that the 13 K cusp in $M_{\mathrm{dc}}(T)$ is a feature of $M_{\mathrm{Cu}}(T)$ rather than the Pr magnetism.

The exact nature of the 13 K $M_{\mathrm{dc}}(T)$ cusp is uncertain at this point. However, two likely candidates are a Cu spin reorientation as suggested by Felner *et al.*[9] or a coupling of the Cu WF to an AF Pr ordering. There is no evidence of a spin structure transition in the neutron-diffraction or $M_0(T)$ data for PrCSCNO. But the $M_0(T)$ data do show an reduction of its slope below 20 K which is consistent with an expected weakening of the Cu WF due to coupling to an AF Pr ordering. Furthermore, the 13 K $M_{\mathrm{dc}}(T)$ cusp occurs at a temperature higher than the 7 K $\chi_d(T)$ cusp, which is consistent with the Cu WF coupling to the developing long-range AF ordering above T_N in the Pr sublattice. Hence, we favor Cu-Pr coupling as a possible source of the 13 K cusp.

We mention that in our earlier work we attributed the 13 K $M_{\mathrm{dc}}(T)$ cusp to an ordering of Pr moments,[6] while Felner *et al.* attributed it to a reorientation of the Cu moments and suggested that there is no ordering of the Pr moments in PrCSCNO.[9] Our present results indicate neither interpretation was correct. Although the $\chi_d(T)$ data are consistent with an ordering of the Pr spins in PrCSCNO, the 7 K $\chi_d(T)$ cusp is not observable in the $M_{\mathrm{dc}}(T)$ data since the contribution of the Cu magnetism to the $M_{\mathrm{dc}}(T)$ data eclipses the Pr magnetism. Furthermore, it is apparent that the 13 K cusp originates from the Cu magnetism. Finally, the data do not support a reorientation of the Cu moments as the origin of the 13 K cusp, but are consistent with a coupling of the WF behavior to a Pr ordering.

Field-cooled and zero-field-cooled $M_{\mathrm{dc}}(T)$ data at $H=10$ Oe for PrCSCTO are shown in Fig. 4(b). The data show irreversibilities and a low-temperature cusp at 20 K similar to those in $M_{\mathrm{dc}}(T)$ data for PrCSCNO. $M_{\mathrm{dc}}(H)$ data also show hysteresis and relaxations identical to those of PrCSCNO. These results indicate similar magnetisms in these compounds. However, there is nothing in the data that represents a counterpart to the 57 K cusp in the PrCSCNO data. This indicates that the 57 K spin structure transition in PrCSCNO is absent in PrCSCTO. More recent magnetic analysis on the $(Pr_{1.5}Ce_{0.5})Sr_2Cu_2(Nb_{1-y}Ta_y)O_{10-\delta}$ system suggests that the 57 K transition may still be present in PrCSCTO but is suppressed to lower temperatures where it occurs concurrently with another low-temperature cusp comparable to the 13 K cusp in the data of Fig. 4(a) to yield the observed 20 K cusp.[23] $\chi_d(T)$ and $M_0(T)$ data for PrCSCTO were obtained in the same manner as for PrCSCNO and are shown in the insets of Fig. 5. The $\chi_d(T)$ data are identical to that for PrCSCNO and show a cusp below 10 K with an apex

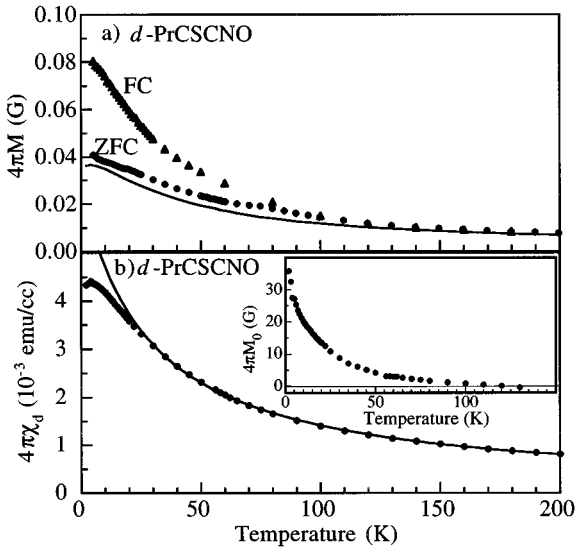

FIG. 7. (a) Zero-field-cooled and field-cooled $M_{\mathrm{dc}}(T)$ data at $H=10$ Oe for d-PrCSCNO—the solid line is the contribution of the Pr ions calculated from $\chi_d(T)$. (b) Differential susceptibility and $M_0(T)$ (inset) data for d-PrCSCNO—the solid line represents the Curie-Weiss fit of the $\chi_d(T)$ data.

at ~7 K. The $\chi_d(T)$ data for 40 K$<T<$200 K were fit to a Curie-Weiss profile and the results are summarized in Table III. The values of the fit parameters are essentially identical to those for PrCSCNO. These results indicate that the Pr magnetism of PrCSCTO is comparable to that of PrCSCNO and that the Pr magnetism of PrCSCNO is unaffected by the substitution of Ta for Nb. The $M_0(T)$ data likewise show similar behavior to that of PrCSCNO both in magnitude and profile but with no features near 57 K, reflecting the behavior of the $M_{\mathrm{dc}}(T)$ data in Fig. 4(b). This indicates that aside from the 57 K transition, PrCSCNO and PrCSCNO have similar Cu magnetism. It is not surprising that isostructural PrCSCNO and PrCSCTO exhibit similar magnetic properties since the Pr and Cu crystallographic sites are relatively far removed from the Nb/Ta sites and the Nb and Ta ions presumably have the same oxidation state and comparable ionic radii. The primary effect of substitution of Nb by Ta appears to be a slight change in the lattice parameters (Table I) and a suppression of the 57 K transition. This indicates that the 57 K spin structure transition in PrCSCNO may be sensitive to the structural parameters of the lattice.

Field-cooled and zero-field-cooled $M_{\mathrm{dc}}(T)$ data at $H=10$ Oe for d-PrCSCNO are shown in Fig. 7(a) and are similar to d-PrCSCNO $M_{\mathrm{dc}}(T)$ results reported by Felner *et al.*[9] Although the data show that the irreversibilities seen in the data for PrCSCNO are still present, they are considerably weaker and both the 13 and 57 K cusps are absent. $\chi_d(T)$ and $M_0(T)$ data were collected as for PrCSCNO and are shown in Fig. 7(b). The d-PrCSCNO $\chi_d(T)$ data are identical to those for PrCSCNO in terms of magnitude, profile, and a cusp at ~7 K. The results of a fit of the $\chi_d(T)$ data for 40 K$<T<$200 K to $\chi_0+C/(T-\theta)$ are shown in Table III and indicate that the Pr magnetism of PrCSCNO is unaffected by removal of oxygen from the lattice. In contrast, the $M_0(T)$ data for d-PrCSCNO are considerably weaker than that of PrCSCNO and show only a diminished feature near 57 K

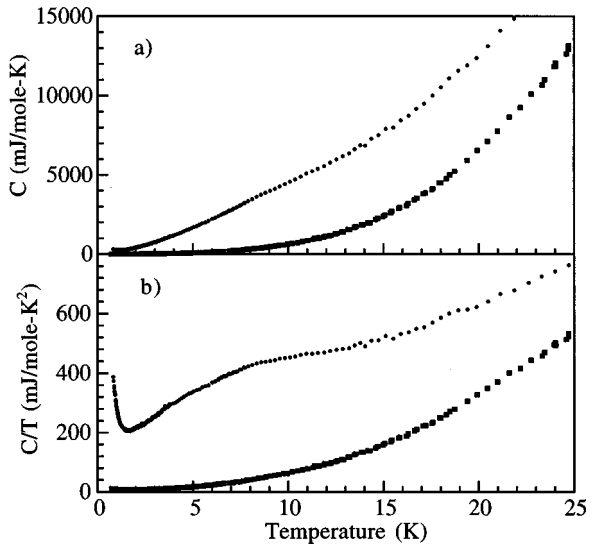

FIG. 8. Specific-heat data for EuCSCNO (■) and PrCSCNO (●) in terms of (a) C vs T and (b) C/T vs T.

indicating that the Cu WF and the 57 K transition are suppressed by the removal of oxygen from the lattice. The insensitivity of the Pr magnetism and contrasting sensitivity of the Cu magnetism to the removal of oxygen from the lattice indicate that the suppression of the 57 and 13 K cusps are associated with the resulting modification of the Cu magnetism. This corroborates the above determination that the 13 and 57 K features in the PrCSCNO $M_{\rm dc}(T)$ data are due to the contribution of the Cu magnetism and not the Pr magnetism. Finally, the expanded lattice for d-PrCSCNO suggests that the PrCSCNO WF behavior and the 13 and 57 K $M_{\rm dc}(T)$ cusps are sensitive to the structural parameters of the lattice in agreement with the above analysis of the magnetic properties of PrCSCTO.

Field-cooled and zero-field-cooled $M_{\rm dc}(T)$ data at $H=10$ Oe for d-PrCSCTO show that upon deoxygenation of PrCSCTO, the 20 K $M_{\rm dc}(T)$ cusp is suppressed and the irreversibilities are weakened. These deoxygenation effects are similar to those seen for PrCSCNO. $\chi_d(T)$ data for d-PrCSCTO are identical to that for PrCSCTO and show the same low-temperature cusp, comparable Curie-Weiss fit parameters (Table III), and reduced Pr $\mu_{\rm eff}$ as $\chi_d(T)$ data of PrCSCTO and PrCSCNO. As expected, the $M_0(T)$ data for d-PrCSCTO are significantly weaker than that from PrCSCTO. These results indicate that the effect of the removal of oxygen from the lattice in PrCSCTO are analogous to that for PrCSCNO—further indicating cognate magnetic properties and mechanisms for these two compounds.

Specific-heat data between 0.6 and 25 K for EuCSCNO and PrCSCNO in terms of $C(T)$ and $C(T)/T$ are shown in Figs. 8(a) and 8(b). The data for EuCSCNO agree with previously reported results[9] and are similar to those for both EuBCO and YBCO.[24–26] Below 1 K there is shallow upturn in the $C(T)/T$ data analogous to that seen for EuBCO and YBCO,[24–26] whose origin is not fully understood. Additionally, near 27 K no anomaly associated with a superconducting transition can be discerned due to a combination of factors which may include: (i) a large lattice specific heat drowning out the electronic specific heat at this elevated temperature, (ii) a small superconducting volume fraction near T_C due to inherent inhomogeneities in the critical parameters of T_C, and (iii) a broad distribution of electronic entropy away from T_C due to the d-wave or anisotropic s-wave superconducting state proposed for high-T_C cuprates. These and other reasons are discussed in detail elsewhere.[24,25] Following standard practice for high-T_C cuprates,[24] the data for EuCSCNO were fit to the analytical expression $C(T)=\alpha/T+\gamma T+\beta T^3+\delta T^5$ for 0.6 K$<T<$13 K. α/T is used to model the shallow upturn below 1 K so that other parameters would not be overestimated, γ is the Sommerfeld constant, and βT^3 and δT^5 are the Debye and anharmonic lattice specific heats. The fit yielded values of 3.2(1) mJ/mole for α, 4.66(9) mJ/mole K^2 for γ, 0.498(5) mJ/mole K^4 for β, and $7.2(3)\times10^{-4}$ mJ/mole K^6 for δ with a χ^2_ν of 0.341. The low value of γ is typical for high-T_C cuprates with low impurity levels,[24,27] the value for β yields a Debye temperature θ_D of 405(1) K which is comparable to the accepted values for high-T_C cuprates,[24,27] and δ is small as expected. From 10 to 60 K, $C(T)$ data were found to fit well to the expression $C_P=4.66T+P_5(T)$, where $4.66T$ is the low-temperature linear term found above and $P_5(T)$ is a fifth-order polynomial used to model the lattice specific heat which is complex in this temperature region.

The $C(T)$ data for PrCSCNO [Fig. 8(a)] are similar to those previously reported by Felner *et al.*[9] with no clear magnetic anomaly below 20 K. However, the $C(T)/T$ data in Fig. 8(b) show a broad but clear anomaly centered near 10 K. This situation is similar to that for the $(Y_{1-x}Pr_x)$BCO and $(Eu_{1-x}Pr_x)$BCO systems with x near 0.75 (i.e., substitutional disorder of the Pr sublattice comparable to PrCSCNO) where the magnetic anomaly associated with the Pr T_N is not obvious in $C(T)$ data but clearly visible in $C(T)/T$ data.[25,26] The breadth and shallowness of the 10 K anomaly is therefore of no surprise—even more so in this case because of the additional disorder introduced in the crystal fields at the Pr site from the random substitution of a Ce^{+4} ion for a Pr^{+3} ion. Hence, in these dilute magnetic systems, interpretation of magnetism through $C(T)$ data is not straightforward. This 10 K anomaly in the $C(T)/T$ data corresponds to the 7 K cusp in the χ_d data of Fig. 5 and is consistent with a magnetic long-range ordering of the Pr sublattice indicated in the PrCSCNO magnetic data. Other features in the $C(T)/T$ data include a sharp upturn below 1 K—indicative of a nuclear Schottky anomaly, and considerable entropy associated with the substitution of Pr for Eu.

The PrCSCNO $C(T)$ data are modeled as $C(T)=C_l(T)+C_{\rm mag}(T)+C_n(T)$ where $C_l(T)$ represents the lattice specific heat, $C_{\rm mag}(T)$ is the magnetic specific heat due to the Pr ions, and $C_n(T)$ is a nuclear Schottky anomaly. $C_l(T)$ is approximated as the lattice specific heat of isostructural EuCSCNO found from the above fits, and $C_n(T)$ is approximated as the usual high-temperature tail of a nuclear Schottky anomaly, AT^{-2}. Attempts were made to fit low-temperature $\Delta C(T)=C(T)-C_l(T)=AT^{-2}+C_{\rm mag}(T)$ data ($T<2$ K) for various analytical forms for $C_{\rm mag}(T)$ which included two-dimensional exponential or three-dimensional cubic magnon terms both with and without an enhanced Sommerfeld-type linear term like that found in PrBCO. As with PrBCO, the only form for $C_{\rm mag}(T)$ which fit the data well was the cubic magnon term, MT^3, plus a linear term,

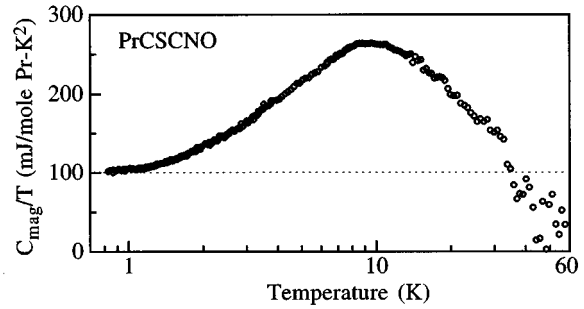

FIG. 9. The magnetic contribution to the specific heat of PrCSCNO.

γT. A fit of $\Delta C(T)$ data for 0.6 K$<T<$2.0 K to the analytical expression $\Delta C(T)=AT^{-2}+MT^3+\gamma T$ yielded values of 99(1) mJ/mole Pr K^2 for γ, 7.3(6) mJ/mole Pr K^4 for M, and 80(1) mJ K/mole Pr for A with an χ^2_ν of 11.7. The large value for γ is unexpected since PrCSCNO is insulating. However, its entropy is clearly associated with the Pr ions, and it is both similar to the enhanced γ's in heavy-fermion compounds and comparable to the large γ of 100 mJ/(mole Pr K^2) reported for PrBCO.[1,3,24–26] The value for A yields a hyperfine field $H_{\rm hf}$ of 92(1) T, also comparable to the $H_{\rm hf}$ found for PrBCO.[3]

Once $C_n(T)$ was determined from the data fits, the magnetic specific heat $C_{\rm mag}(T)$ was computed from $C_{\rm mag}(T)=\Delta C(T)-C_n(T)=C(T)-C_l(T)-C_n(T)$ and is shown in Fig. 9. The magnetic peak in the data is centered at 10 K and is prominent. The entropy $S_m(T)$ (per Pr ion) associated with $C_{\rm mag}(T)$ was computed by numerical integration of $C_{\rm mag}(T)/T$ data and from a linear extrapolation of $C_{\rm mag}(T)/T=MT^3+\gamma T$ below 0.6 K, where values for M and γ come from the above fits. The results are shown in Fig. 10. $S_m(T)$ asymptotically approaches R ln(3) with increasing T which is consistent with the $J=1$ Hund's rules ($^3H_4$) ground state for a $+3$ valence Pr ion. This confirms the $+3$ valence state for the Pr ion in PrCSCNO found with EELS and other measurements.[5,10–12] Finally, we point out that the thermal distribution of $S_m(T)$ is comparable to that for PrBCO.[3] This corroborates the indication by the reduced Pr $\mu_{\rm eff}$ found from the $\chi_d(T)$ data of Fig. 5 that the Pr $4f$ CF scheme of PrCSCNO is comparable to that of PrBCO.

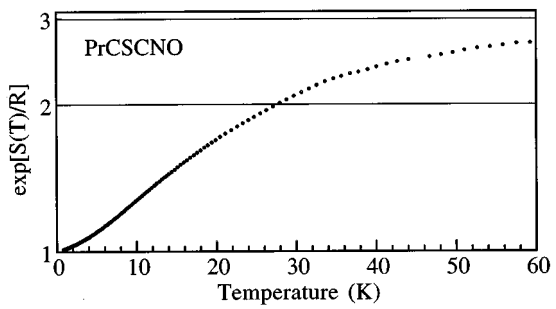

FIG. 10. Temperature dependence of the entropy of the magnetic specific heat of PrCSCNO.

IV. DISCUSSION AND CONCLUSION

The results of our measurements and analyses on PrCSCNO indicate a Cu magnetic state marked by AF order of the Cu spins with a T_N above 200 K and three distinct spin structures in the temperature regions from the T_N (just above 200 K) down to 130 K (phase I), 130–57 K (phase II), and below 57 K (phase III). The properties of phase I are consistent with either a $+--+$ or $++++$ collinear spin structure as described above. Phases II and III, however, show noncollinear spin structures in conjunction with WF behavior. The spin configurations of the noncollinear spin structures and their relationships to the WF behavior are uncertain at this point and will be the subject of further study. The transitions between these phases are manifested by (i) an onset of magnetic peaks in the neutron-diffraction data at the T_N ($>$200 K) for the beginning of phase I, (ii) a redistribution of the magnetic peak intensities and an onset of WF behavior in the magnetic data at the transition from phase I to II near 130 K, and (iii) a redistribution of magnetic peak intensities and a cusp in the magnetization data at the transition from phase II to III at 57 K. In addition, the features in the magnetic data which we attribute to the Cu magnetism appear to dominate the $M_{\rm dc}(T)$ of PrCSCNO below $\sim$80 K and overshadow the contribution of the Pr magnetism. These features include: (i) WF behavior that leads to large irreversibilities and relaxations in the $M_{\rm dc}$ data below 130 K, (ii) a cusp in the $M_{\rm dc}(T)$ data at 57 K that appears to be the magnetic signature of the transition between phases II and III, and (iii) a cusp at 13 K in the $M_{\rm dc}$ data whose origin is not clear but which may be due to Cu-Pr coupling. The microscopic origin of the WF in PrCSCNO and its relationship to the crystal structure is uncertain at this time. However, this WF appears to be analogous to that observed in some of the R_2CuO_4 T' structured cuprates. This analogy serves as a basis for our interpretation and analysis of the magnetic data of PrCSCNO and allows us to distinguish between the contributions of the Cu and Pr magnetisms to the $M_{\rm dc}(T)$ data. The appropriateness of these analyses is substantiated not only by the similarities of the structures and properties of the RCSCNO and T' compounds, but by the self-consistency of our results and the expected results for this class of compounds. As a final comment on the Cu magnetism in PrCSCNO, we point out that our interpretation of the WF behavior makes the exact crystal structure and issue of local distortions of the lattice relevant to understanding the magnetic state of PrCSCNO.

The results for PrCSCNO also indicate that the Pr sublattice has a T_N near 10 K. We compare this T_N to those reported for other RCSCNO compounds; NdCSCNO ($<$1.4 K),[27] SmCSCNO (4.5 K),[28] and GdCSCNO (5.5 K).[29] From a scaling of these rare-earth ordering temperatures, in a manner similar to the scaling performed for the RBCO compounds,[1,25] we see that the Pr T_N is roughly an order of magnitude larger than expected. This anomalously large T_N for PrCSCNO suggests that the rare-earth magnetic interactions in PrCSCNO are of a different nature than for the other RCSCNO compounds. Furthermore, a reduced Pr $\mu_{\rm eff}$, the thermal distribution of $4f$ entropy, and an enhanced linear contribution to the low-temperature specific heat for

PrCSCNO indicate that the Pr $4f$ CF ground state is comparable to that of PrBCO. These remarkable similarities between the behavior of the Pr magnetism for PrBCO and PrCSCNO indicate that their underlying mechanisms are of the same nature. As with PrBCO,[1] the magnitude of the Pr T_N, the insulating state, and the Pr-Pr distance suggest that a dipole-dipole, Ruderman-Kittel-Kasaya-Yosida, and direct exchange interaction are not viable mechanisms for the Pr-Pr magnetic interactions in PrCSCNO. This and the similarities between PrCSCNO and PrBCO suggest that Pr magnetism in PrCSCNO is mediated by a superexchange interaction, probably though the nearest-neighbor oxygen ions.

Upon deoxygenation of PrCSCNO, the lattice expands and those features in the magnetic data which we attribute to the Cu magnetism—WF behavior and the 13 and 57 K cusps—are weakened or suppressed while the Pr magnetism is relatively unchanged. These results indicate that oxygen stoichiometry is a critical parameter of the Cu magnetism in PrCSCNO. The mechanism behind this relationship is uncertain, but either the Cu-O spacing or disorder in the occupancy of crystallographic oxygen sites are suspected. Finally, the magnetic properties of PrCSCTO and *d*-PrCSCTO indicate that they have identical Pr magnetism and similar Cu magnetism as PrCSCNO and *d*-PrCSCNO. This indicates that substitution of Ta for Nb in PrCSCNO leaves the underlying magnetic mechanisms of these materials relatively intact.

It is interesting to note that the properties of PrCSCNO (and PrCSCTO) can be understood in terms of properties of the *R*BCO and R_2CuO_4 T' compounds on several levels. First, the crystal structure of PrCSCNO can be seen as a combination of the *R*BCO and R_2CuO_4 T' structures.[5,6,10,11] The R_2O_2 fluorite layers of PrCSCNO sandwiched between the CuO_2 planes represents a T'-like substructure while the intermediate SrO-NbO_2-SrO layers are reminiscent of the BaO-CuO-BaO layers of the *R*BCO structure. Second, Pr appears to induce the same anomalous effects in the *R*CSCNO structure as in the PrBCO structure—suppressing superconductivity, bringing about an insulating electronic state, and showing anomalous Pr magnetism. Third and last, PrCSCNO shows a Cu magnetism marked by WF behavior like that observed in some of the R_2CuO_4 T' cuprates. From these observations, it becomes clear that the complex properties of PrCSCNO (and PrCSCTO) can be understood simply as a melding of properties and mechanisms that are already known and well characterized in high-T_C cuprates.

These results indicate that there are now three structurally related Pr-containing high-T_C compounds—PrBCO, PrCSCNO, and PrCSCTO—in which superconductivity is suppressed in the same phenomenological manner. These compounds are unexpectedly nonsuperconducting, exhibit an unexplained electronic insulating state, and show remarkably similar anomalous Pr magnetism and CF ground states. In high-T_C compounds where the presence of Pr does not affect superconductivity, such as $(Pr_{1.83}Ce_{0.17})CuO_4$ or $Bi_2Sr_2(Ca_{1-x}Pr_x)Cu_2O_8$, Pr does not show anomalous magnetism and the Pr ion has a conventional singlet CF ground state.[1] This indicates that a suppression of superconductivity and anomalous Pr magnetism occur together or not at all and are therefore correlated. This also indicates that an unexpected insulting electronic state, a pseudotriplet Pr $4f$ CF ground state, and a large linear contribution to the low-temperature specific heat are characteristic of and intimately related to the suppression of superconductivity and anomalous Pr magnetism in these materials. We therefore propose that: (1) there exists a subclass of high-T_C compounds which are Pr-based and characterized by an unexpected lack of superconductivity, an unexpected insulating electronic state, anomalous Pr magnetism, and a pseudotriplet Pr $4f$ CF ground state; (2) a general correlation exists between the suppression of superconductivity by the Pr ion and the anomalous Pr magnetism; and (3) by generalizing this phenomena, we likewise generalize the models, mechanisms, and controversies surrounding PrBCO and extend them to both PrCSCNO and PrCSCTO.

The existence of a subclass advances our understanding of these materials by providing a general description of this phenomenon independent of any one system. This yields concise criteria for understanding and modeling these compounds by requiring that any viable model for the suppression of superconductivity must explain the relationship of the Pr magnetism and other anomalous properties to the suppression of superconductivity. This also discharges material specific properties not directly associated with this phenomenon which would otherwise mislead our preception and modeling. For example, the CuO chains of the *R*BCO structure play an key role in determining the transport properties of the *R*BCO compounds. However, the absence of the chains in *R*CSCNO structure renders the role of the chains as extrinsic to the mechanism behind the suppression of superconductivity and other anomalous properties of these Pr-based compounds. Finally, we point out that the existence of the proposed subclass of compounds is also supported, though less definitely, by the properties of the $PrBa_2Cu_2NbO_8$,[30] $TlBa_2PrCu_2O_7$,[31] $Pb_2Sr_2PrCu_3O_8$,[32] $CmBa_2Cu_3O_7$,[33] and $Pb_2Sr_2CmCu_3O_8$ (Ref. 34) compounds.

The exact origin of the correlation between the suppression of superconductivity and anomalous Pr magnetism is unclear at this time. However, this correlation suggests either a shared underlying mechanism or that one phenomenon directly leads to the other. In the former case, a mechanism of interest is the hybridization-localization model often discussed in the literature for PrBCO,[1,4] where interactions between the Pr $4f$ and CuO_2 planar electronic states both mediate a Pr magnetic interaction and localize conduction electrons, thereby suppressing superconductivity. In the latter case, pair breaking where the Pr magnetism suppresses superconductivity by scattering Cooper pairs is the relevant mechanism.[1,4] The merits and soundness of these and other models are discussed in detail elsewhere.[1,4,11,13] However, we point out that the relevance of the models for PrBCO to PrCSCNO bring up several important issues regarding the properties of PrCSCNO (and PrCSCTO) that should be addressed in order to solidify our proposals. First, there is no hard evidence for the existence of f-electronic interactions in PrCSCNO. Hence, we rely upon the inference of f-electron interactions by the anomalous Pr magnetism[1] and upon the strength of our proposal of a generalization of the phenomenon surrounding the suppression of superconductivity in Pr-based cuprates. Second, there is little information about the

mechanism behind the suppression of superconductivity in PrCSCNO. We mention, however, that our recent results for the $(R_{1.5-x}Pr_xCe_{0.5})Sr_2Cu_2NbO_{10-\delta}$ R=Nd, Sm, Eu series of compounds indicate that as with PrBCO, a conventional Abrikosov-Gor'kov pair breaking does not appear to adequately model the suppression of superconductivity by the Pr ion in the RCSCNO structure.[11,13]

ACKNOWLEDGMENTS

The authors gratefully acknowledge support for this work from the National Science Foundation under Grant No. DMR-94-03895 and Lawrence Livermore National Laboratory under the auspices of the U.S. Department of Energy through Contract No. W-7405-ENG-48.

[1] H. B. Radousky, J. Mater. Res. **7**, 1917 (1992), and references therein.

[2] L. Soderholm, C-K. Loong, G. L. Goodman, and B. D. Dabrowski, Phys. Rev. B **43**, 7923 (1991); G. L. Goodman, C-K. Loong, and L. Soderholm, J. Phys. Condens. Matter **3**, 49 (1991).

[3] N. E. Phillips, R. A. Fisher, R. Caspary, A. Amato, H. B. Radousky, J. L. Peng, L. Zhang, and R. N. Shelton, Phys. Rev. B **43**, 11 488 (1991); R. A. Fisher, N. E. Phillips, D. A. Wright, H. B. Radousky, T. J. Goodwin, J. L. Peng, and R. N. Shelton, Physica B **194**, 469 (1994), and references therein.

[4] D. Khomskii, J. Supercond. **6**, 69 (1993), and references therein; Y. Imanaka, K. Tamasaku, T. Ito, and S. Uchida, Phys. Rev. B **46**, 5833 (1992).

[5] Li Rukang, Zhu Yingjie, Qian Yitai, and Chen Zuyao, Physica C **176**, 19 (1991); Li Rukang, Zhu Yingjie, Xu Cheng, Chen Zuyao, Qian Yitai, and Fan Chengao, J. Solid State Chem. **94**, 206 (1991).

[6] T. J. Goodwin, H. B. Radousky, and R. N. Shelton, Physica C **204**, 212 (1992).

[7] R. J. Cava, J. J. Krajewski, H. W. Zandbergen, R. B. Dover, W. F. Peck, Jr., and B. Hessen, Physica C **191**, 237 (1992).

[8] Wang Shiwei, Qian Yitai, Li Rukang, Chen Zuyao, Wang Nanlin, Cao Liezhao, Zhou Guien, and Zhang Yuheng, Physica C **210**, 463 (1993).

[9] I. Felner, U. Yaron, U. Asaf, T. Kröner, and V. Breit, Phys. Rev. B **49**, 6903 (1994).

[10] T. J. Goodwin, H. B. Radousky, and R. N. Shelton, J. Solid State Chem. (to be published).

[11] T. J. Goodwin, Ph.D. thesis, University of California, Davis, 1995.

[12] S. C. Cheng, V. P. Dravid, T. J. Goodwin, R. N. Shelton, and H. B. Radousky, Phys. Rev. B **53**, 11 779 (1996).

[13] T. J. Goodwin, M. D. Lan, H. B. Radousky, and R. N. Shelton (unpublished).

[14] J. W. Lynn, in *High Temperature Superconductivity*, edited by J. W. Lynn (Springer-Verlag, New York, 1990).

[15] S-W. Cheong, J. D. Thompson, and Z. Fisk, Phys. Rev. B **39**, 4395 (1989).

[16] S. B. Oseroff, D. Rao, F. Wright, D. C. Vier, S. Schultz, J. D. Thompson, Z. Fisk, S-W. Cheong, M. F. Hundley, and M. Tovar, Phys. Rev. B **41**, 1934 (1990), and references therein.

[17] M. Tovar, X. Obradors, F. Pérez, S. B. Oseroff, R. J. Duro, J. Rivas, D. Chateigner, P. Bordet, and J. Chenavas, Phys. Rev. B **45**, 4729 (1992), and references therein.

[18] A. Rouco, X. Obradors, M. Tovar, F. Pérez, D. C. Hateigner, and P. Bordet, Phys. Rev. B **50**, 9024 (1994), and references therein.

[19] I. Dzyaloshinsky, J. Phys. Chem. Solids **4**, 241 (1958); T. Moriya, Phys. Rev. **120**, 91 (1960).

[20] D. Coffey, K. S. Bedell, and S. A. Trugman, Phys. Rev. B **42**, 6509 (1990); D. Coffey, T. M. Rice, and F. C. Zhang, *ibid*. **44**, 10 112 (1991); and references therein.

[21] H. W. Zandbergen, R. J. Cava, J. J. Krajewski, and W. F. Peck, Jr., Physica C **192**, 237 (1992); **196**, 252 (1992).

[22] A. H. Cooke, D. M. Martin, and M. R. Wells, J. Phys. **7C**, 3133 (1974).

[23] M. Bennahmias, H. B. Radousky, C. N. Buford, A. Kebede, M. McIntyre, T. J. Goodwin, and R. N. Shelton, Phys. Rev. B **53**, 2773 (1996).

[24] R. A. Fisher, J. E. Gordon, and N. E. Phillips, J. Supercond. **1**, 231 (1988), and references therein.

[25] A. Kebede, C-S. Jee, J. Schwegler, J. E. Crow, T. Mihalisin, G. H. Myer, R. E. Solomon, P. Schlottmann, M. V. Kuric, S. H. Bloom, and R. P. Guertin, Phys. Rev. B **40**, 4453 (1989); S. Ghamaty, B. W. Lee, J. J. Neumeier, G. Nieva, and M. B. Maple, *ibid*. **43**, 5430 (1991).

[26] G. Nieva, S. Ghamaty, B. W. Lee, M. B. Maple, and I. K. Schuller, Phys. Rev. B **44**, 6999 (1991).

[27] N. Rosov and J. W. Lynn (unpublished).

[28] N. Brnicevis, I. Basic, P. Planicic, B. Grzeta, M. Tonkovic, M. Forsthuber, G. Hilscher, T. Holubar, H. Michor, H. Kirchmayr, and G. Schaudy, Appl. Supercond. **1**, 519 (1993).

[29] G. Hilscher, T. Holubar, H. Michor, G. Schaudy, H. Kirchmayr, N. Brnicevis, I. Basic, P. Planicic, B. Grzeta, M. Vybornov, and P. Rogl, Physica B **194-196**, 2243 (1994).

[30] M. Bennahmias, J. C. O'Brien, H. B. Radousky, T. J. Goodwin, P. Klavins, J. M. Link, C. A. Smith, and R. N. Shelton, Phys. Rev. B **46**, 11 986 (1992); N. Rosov, J. W. Lynn, H. B. Radousky, M. Bennahmias, T. J. Goodwin, P. Klavins, and R. N. Shelton, *ibid*. **47**, 15 256 (1993).

[31] C. C. Lai, B. S. Chiou, Y. Y. Chen, J. C. Ho, and H. C. Ku, Physica C **202**, 104 (1992).

[32] J. H. Shieh, H. C. Ku, and J. C. Ho, Phys. Rev. B **50**, 3288 (1994).

[33] L. Soderholm and C.-K. Loong, J. Alloys Comp. **193**, 125 (1993).

[34] J. Simon Xue, C. W. Williams, and L. Soderholm, J. Appl. Phys. **75**, 6740 (1993).